Theoretical studies of ion neutralization at a solid surface

Joel A. Appelbaum and D. R. Hamann
Bell Laboratories, Murray Hill, New Jersey 07974
(Received 4 August 1975)

Calculations are presented of the kinetic-energy distribution of Auger electrons emitted during ion neutralization at Si (111) and H-covered Si (111) surfaces. An expression is derived for the Auger electron kinetic-energy distribution (KED) using an "internal" absorption or radiation formulation of the Auger process. This expression relates the KED spectra to various surface electronic densities of states. It includes nonadiabatic energy transfer broadening, but in other respects it is similar to previously derived expressions for KED spectra. The position-dependent density of states for Si (111) and H-covered Si (111) is calculated using a fully self-consistent surface potential. Using these state densities we show that the experimentally measured KED spectra can be reproduced assuming that the Auger electron originates in a region within the last few planes of atoms, while the ion is neutralized a few angstroms outside the last plane. The importance of electron correlations for narrow half-filled surface-state bands is demonstrated and evidence presented that hole-hole interaction energies can be neglected in the neutralization event.

I. INTRODUCTION

The Auger neutralization of slowly moving ions incident on a solid surface has been developed during the last twenty years into a tool for exploring the electronic spectrum of ordered surfaces.[1-2] As such the tool has been known as ion-neutralization spectroscopy—INS.[3-4] Its basic goal has been to take the measured kinetic energy distribution of Auger emitted electrons (KED) and process that information so as to obtain an effective surface density of states. Analysis of the physical assumptions underlying the method have proceeded along a number of lines. Extensive internal consistency checks have been made involving a variety of ion species, kinetic energies, etc. Comparison between extracted surface densities of states and theoretically calculated bulk densities of states as well as with physically plausible spectral models in the case of ordered chemisorbed systems have been made.[5-6] Recently, experimental comparison between the results of INS and ultraviolet photoemission measurements have yielded interesting insights into the respective sensitivities of these two probes to surface electronic properties.[7]

In this paper we take a somewhat different approach to analyzing the Auger neutralization data, or KEDs. Rather than attempting to extract a surface density of states from them we shall use the results of recently available self-consistent field calculations for clean and hydrogenated Si(111) surfaces[8-9] to explain the measured KEDs for these systems. In the process we shall gain additional information concerning the spatial regions from which the neutralizing and emitted electrons come. In addition, the important role electron correlations play for surface states on clean Si(111) will be emphasized.

The remainder of the paper is organized as follows. In Sec. II we review the basic physical processes involved in the ion-neutralization processes, and derive an expression for the Auger electron current. In Sec. III we present the results of calculations of the surface density of states for clean and H-covered Si(111) and use them to explain the experimentally measured KED spectra. The role of electron correlations and matrix-element effects are also considered in this section. Finally, we summarize our conclusion concerning the ion-neutralization process in Sec. IV.

II. BASIC FORMULAS

We review in this section the basic physical processes involved in ion neutralization, following the work of Hagstrum.[1,10] The ions, usually He^+ or Ne^+, travel at velocities $\approx 1\times10^6$ cm/sec toward the surface being studied. For the surfaces of most materials, the direct resonant neutralization of the ion is energetically forbidden and two-electron (Auger) neutralization predominates.[1] In deriving an expression for the Auger-electron-current density, we adopt a multistep view of the process involved in ion neutralization.

As the ion approaches the surface an electronic transition can occur in which an electron from the solid makes a virtual transition to the unoccupied ion ground state, emitting a longitudinal photon. The photon "propagates" towards the surface, capable of exciting an electron anywhere along its trajectory. From this perspective ion neutralization acts to produce a longitudinal photon akin to the transverse photon of photoemission.[11,12] Both are capable of producing an excited electron above the vacuum level, which may escape and be measured. This description of ion neutralization parallels the theory of the atomic Auger process viewed as an internal-conversion event.[13] Two differences exist

between the photons which need emphasis. The first involves their propagation range as they penetrate the solid. The transverse photon penetrates deeply into the solid, many hundreds of angstroms, while the longitudinal photon is screened rapidly by the solid so its penetration is limited to a few angstroms. This makes it an extremely surface-sensitive probe. The second difference involves the coupling of the two photon fields to the excited electrons. The transverse photon couples through the current via an $\vec{A}\cdot\vec{P}$-type interaction while the longitudinal coupling is through the density via a $1/r$ interaction.

Having sketched the processes involved we now write down an expression for the Auger-electron-current density, $N(E_k)$. The effective longitudinal field created by the tunneling electron neutralizing the ion is

$$A_L^{(\vec{x})} \propto \int W(\vec{x}-\vec{x}')\Psi_i(\vec{x}')\Psi_A(\vec{x}')d^3x' \ , \tag{2.1}$$

where $\Psi_i(\vec{x})$ is a metal wave function, $\Psi_A(\vec{x})$ is the ion-ground-state wave function, and $W(\vec{x}-\vec{x}')$ is the propagation kernel for the photon field, i.e., a screened Coulomb interaction potential.[14] Assuming $\Psi_A(x)$ highly localized about the ion nuclear position $\vec{R}$ (2.1) becomes

$$A_L(\vec{x}) \propto W(\vec{x}-\vec{R})\Psi_i(\vec{R})\Psi_A(\vec{R}) \ . \tag{2.2}$$

This longitudinal field has a frequency

$$\hbar\omega = E_i - E_A \ , \tag{2.3}$$

where E_A is the effective ionization energy of the incoming ion and E_i that of the neutralizing electron. Because of the proximity of the ion to the surface, E_A is different from its free-atom limit and depends on R.[15,16] In deriving an excitation rate for electron-hole-pair creation by the longitudinal field $A_L(x)$ it is customary to assume that the perturbation is adiabatically turned on. In the ion-neutralization process this is done by having the ion approach the surface with a constant velocity v_{ion} so that $R_z = R_{0z} - v_{\text{ion}}t$, where R_{0z} is some macroscopic distance measured from the surface such that the incident ion would strike the surface in time $t_0 = R_{0z}/v_{\text{ion}}$ if it were not neutralized. Since

$$\Psi_i(\vec{R}) \approx e^{-\kappa_i R_z} \approx e^{-\kappa_i(R_{0z}-v_{\text{ion}}t)} \ ,$$

and $\hbar\kappa_i v_{\text{ion}} \ll$ (Fermi energy), the perturbing field is turned on slowly.

One has then from first-order time-dependent perturbation theory an excitation rate for producing an electron in state Ψ_e with energy E_e

$$W_e \propto \sum_h |(\Psi_e(x)|A_L(x)|\Psi_h(x))|^2 \frac{\alpha_i}{\alpha_i^2+(E_e-E_h-\hbar\omega)^2} \ , \tag{2.4}$$

where the sum h is over electron states of the solid and α_i is a typical "switch-on" parameter $\sim \kappa_i v_{\text{ion}}$. (For He^+ with kinetic energy 10–100 eV, this corresponds to 0.5–1.0 eV broadening.) The Lorentzian in (2.4) represents in a simple way the possibility of energy exchange between the kinetic energy of the ion and that of the Auger electron. This energy exchange is an inherent source of broadening in the neutralization process.[17] A second source of broadening, the time- and position-dependent shift in the effective ionization energy due to the image potential, is not included in (2.4).

Substituting (2.2) into (2.4) and assuming that $N(E_k)$, the electron current density at energy E_k produced by a neutralization event can be written as a product of an excitation probability W_e and escape probability T_e one obtains

$$N(E_k) \propto \sum_e \delta(E_k-E_e)T_e \sum_{h,i} \frac{\alpha_i}{\alpha_i^2+(E_e-E_h+E_A-E_i)^2} \times \left| \int (\Psi_e(\vec{x})\Psi_i(\vec{R})|W(\vec{x}-R)|\Psi_h(\vec{x})\Psi_A(\vec{R}))d^3x \right|^2 . \tag{2.5}$$

Equation (2.5) represents the contribution to the Auger electron current from a single neutralizing event at position R. There is of course a distribution of R's with weight factors depending on the ion-survival rate. This distribution is, however, sharply peaked at a particular R, dependent of course on the ion velocity.[1] We shall interpret (2.5), evaluated at that most probable R, as representing the total Auger electron current. Rewriting (2.5) one obtains

$$N(E_k) \propto \iiint dE_e\,dE_k\,dE_i\ \delta(E_e+E_A-E_k-E_i)\delta(E_k-E_e) \times M(E_e,E_k;\vec{R})\rho(\vec{R},\vec{R};E_i) \ , \tag{2.6}$$

where

$$M(E_e,E_h;\vec{R}) = \iint d^3x\,d^3x'\,J(\vec{x},\vec{x}';E_e) \times \rho(\vec{x},\vec{x}';E_h)W(\vec{x}-\vec{R})W(\vec{x}'-\vec{R}) \ , \tag{2.7}$$

and

$$\rho(\vec{x},\vec{x}';E) = \sum_i \Psi_i^*(\vec{x})\Psi_i(\vec{x}')\delta(E_i-E)f(E_i) \tag{2.8}$$

is the conventional position-dependent density of occupied states (f is the usual Fermi function) and

$$J(\vec{x},\vec{x}';E) = \sum_i T_i\Psi_i^*(\vec{x})\Psi_i(\vec{x}')\delta(E-E_i)f(E_i) \tag{2.9}$$

is a weighted electron state density, where the weight factor is the flux contributed by the state.

In rewriting (2.5) to obtain (2.6) we have taken the $\alpha_i \to 0$ limit [i.e., ignored nonadiabatic broadening and suppressed $\Psi_A(R)$]. Consider the spatial

integrations in (2.6). The regions of most importance for these integrations depend on R. From studies of the effective ionization energy E_A of the incident ion estimates of R between 2 and 3 Å from the surface plane are obtained. This then places R in the region of exponential decay for occupied wave functions of the solid. The Coulomb interaction $W(\vec{x}-\vec{R})$ is peaked for $\vec{x}=\vec{R}$, decays for $\vec{x}$ approaching the surface layer, and then drops very rapidly as the Coulomb field is screened by the solid. On the other hand, $\rho(\vec{x},\vec{x}';E)$ decays rapidly as $\vec{x}$ or $\vec{x}'$ moves into the vacuum region. The region of dominance for the spatial integrals is therefore determined by a competition between the exponentially decaying $\rho(\vec{x},\vec{x}';E)$ and the growing function $W(\vec{x}-\vec{R})$, $\vec{x}\to$ vacuum. We shall assume that this region is centered at $\vec{x}=\vec{R}^*$, and in Sec. III present evidence that $\vec{R}^*$ is in fact close to or within the surface layer. The integrations on $\vec{x}$ and $\vec{x}'$ are then done simply by replacing in (2.6) $\vec{x}$ and $\vec{x}'$ by $\vec{R}^*$, yielding for $N(E_k)$

$$N(E_k)\propto\int\int\int dE_e\,dE_h\,dE_i\,J(\vec{R}^*,E_e)\rho(\vec{R}^*,E_i)\rho(\vec{R},E_k)\times[W(\vec{R}^*-\vec{R})]^2\delta(E_e-E_h+E_A-E_i)\delta(E_k-E_e)\,, \tag{2.10}$$

where

$$J(\vec{x},E)=J(\vec{x},\vec{x};E) \tag{2.11}$$

and

$$\rho(\vec{x},E)=\rho(\vec{x},\vec{x};E)\,.$$

The above discussion has assumed that all ions approaching the surface neutralize with maximum probability in a given plane. In other words, that $\vec{R}$ can be treated as a scalar quantity. How good an approximation is this? If we assume that an ion incident on the surface with some "impact coordinate" $\vec{R}_{\parallel}$ will neutralize when it encounters an effective electron density ρ_0, then the surface of maximum neutralization is defined by $\rho(R_z,\vec{R}_{\parallel})=\rho_0$. In regions of high density the surface defined above is anything but planar (see Fig. 2 in Ref. 8, for example). However, as the density becomes small the finite $\vec{G}_{\parallel}$ Fourier coefficients $\rho_{\vec{G}_{\parallel}}(z)$ in the expansion of $\rho(z,\vec{x}_{\parallel})$, viz.,

$$\rho(z,\vec{x}_{\parallel})=\sum\rho_{\vec{G}_{\parallel}}(z)\,e^{i\vec{G}_{\parallel}\cdot\vec{x}_{\parallel}}\,,$$

rapidly become small compared to the planar average component, $\rho_0(z)$. $\rho_0(z)$ itself decays rapidly in the low-density vacuum region. The two effects—the rapid variation of $\rho(\vec{x})$ with z and the more rapid disappearance of its variation with $\vec{x}_{\parallel}$—combine to make the surface $\rho(R_z,\vec{R}_{\parallel})=\rho_0$ for $\rho_0\lesssim 1\times10^{-3}$ a.u. relatively planar. Graphic illustration of this effect is contained in Fig. 1.

Performing two of the energy integrals in (2.9) allows us to obtain a final form for $N(E_k)$:

$$N(E_k)\propto J(\vec{R}^*,E_k)\,|\,W(\vec{R}^*-\vec{R})\,|^2\times\int\rho(\vec{R}^*,E-E_i)\rho(\vec{R},E_i)dE_i\,, \tag{2.12}$$

$$E=E_k+E_A\,. \tag{2.13}$$

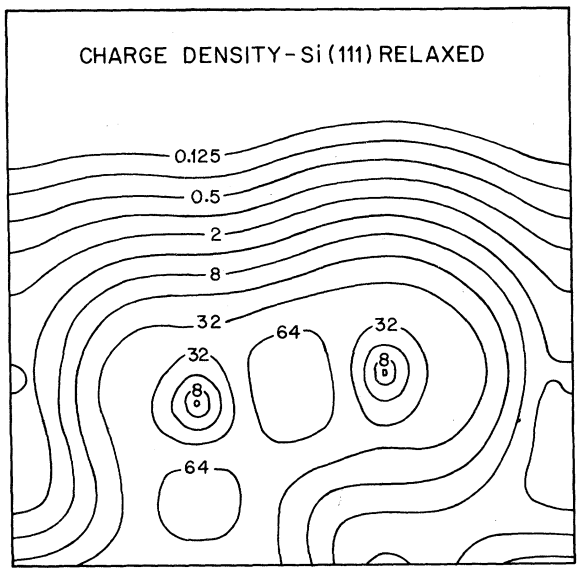

FIG. 1. Contour plot of the charge density for clean Si on a plane normal to the surface and passing through a row of surface atoms and the bond between the first and second atomic layers. Atom positions are indicated by heavy dots, and a geometric progression of contours has been chosen to present detail in the region of low density near the vacuum. The density has been multiplied by 10^3 and is in atomic units.

III. THEORETICAL ANALYSIS

The goal of this section will be to use (2.12) to explain the KED spectra shown in Fig. 2. These data, taken by Sakurai and Hagstrum[18] using 10-eV He^+, show the evolution of the KED for annealed Si(111) with H adsorption. The two limiting curves represent clean Si(111) and H chemisorbed on Si(111) to saturation coverage, assumed here to be a monolayer. It will be these two curves that we shall focus upon.

The theoretical energy distribution $N(E_k)$ is proportional to an escape factor J, a matrix element W, and the crossfold of two position-dependent occupied densities of states. The escape factor J varies slowly with E_k except near vacuum threshold, where $J(E)\to 0$ as $E\to E_{\rm vac}$ (vacuum level). This accounts for the sharp cutoff of $N(E)$ seen in Fig. 2 for $E-E_{\rm vac}\lesssim 3$ eV. Since we shall focus on the region $E-E_{\rm vac}>3$ eV we can treat J, and for that matter W, as constants, so that $N(E)$ is proportional to a convolution of position-dependent

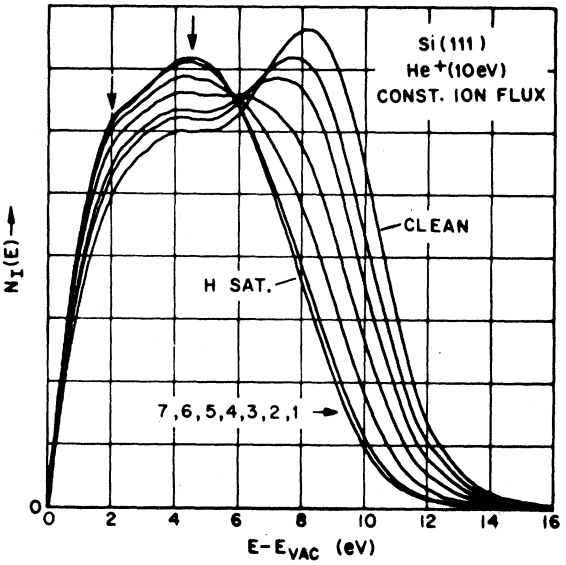

FIG. 2. Experimentally measured kinetic energy distribution $N(E)$, normalized to constant ion flux, is plotted versus energy for clean Si(111) and various exposures (to saturation) of H. The ion used was He^+ at 10 eV kinetic energy (data taken by T. Sakurai and H. D. Hagstrum, Ref. 18).

densities of states.

In attempting to explain the measured KED for clean and hydrogenated Si(111) a knowledge of the position-dependent density of states for these two surfaces is required. These state densities can be obtained from recently completed self-consistent calculations of the electronic structure of clean and hydrogen-covered unreconstructed Si(111).[8,9] While the neutralization measurements were done on the 7×7 reconstructed phase of Si(111), we believe the theoretical information on the unreconstructed surface is appropriate for the following reasons. The 7×7 structure transforms into a 1×1 form at 840 °C in what appears to be a reversible transition,[19] implying that there may not be major structural differences between these two forms of Si. In addition, theoretical predictions for the density of states of clean and hydrogen-covered Si surfaces, assuming no reconstruction, agree in most respects with those inferred from photoemission measurements on the reconstructed surface.[20] Having argued for the relevance of the 1×1 calculations we now discuss the position-dependent densities of states they predict for the surface region.

In Fig. 3(a) we plot the planar average density of states

$$\rho(z, E) = \int \rho(\vec{x}, E) d^2x_{\parallel} ,$$

for relaxed (by 0.34 Å) Si(111) at $z = 1.7$ and 2.8 Å, where $z = 0$ is at the last plane of Si atoms. The histograms were constructed using a limited-surface Brillouin-zone sampling procedure already discussed in the literature.[9] The results of this sampling scheme applied to the bulk are shown in Fig. 3(b). In comparing Fig. 3(a) with Fig. 3(b) it is important to realize that all three curves have been normalized to the same total integrated density in order to exhibit the relative importance of various energy regions for $\rho(z, E)$. $\rho(z, E)$, integrated over all occupied E, decays exponentially with z, as is shown in Fig. 4. Notice how rapidly the density drops off in vacuum. Returning to Fig. 3 one sees that the relative importance of the s-band portion of the spectra is greatly diminished for states within the vacuum and it is only the p bands that survive somewhat intact. Above the valence-band maximum, one has significant weight contributed by the dangling bond surface state band. This state becomes progressively more important

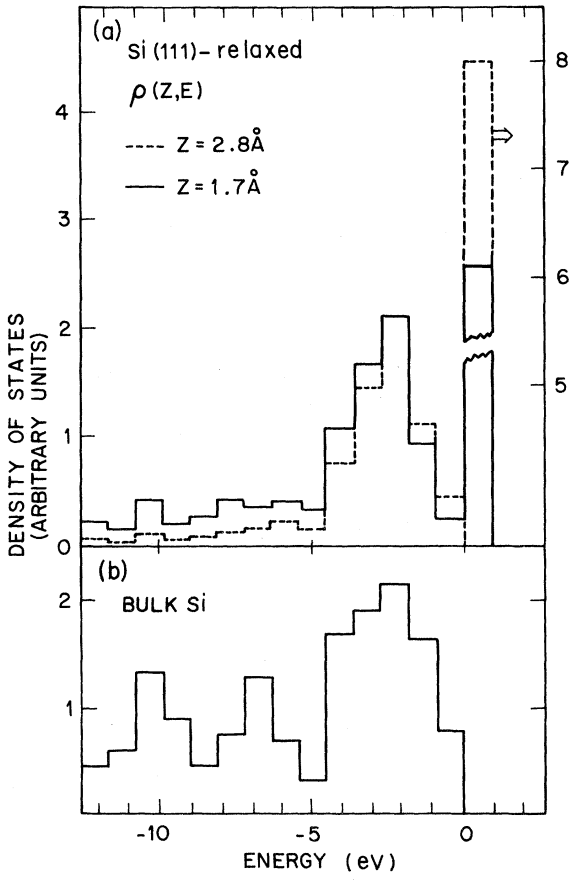

FIG. 3. (a) Planar average density of states for 1×1 relaxed Si(111) surface is plotted versus energy for two positions (relative to the outermost Si atom plane). The zero of energy is taken as the valence-band maximum. Both curves are normalized to constant area. (b) The bulk density of states for Si is plotted versus energy.

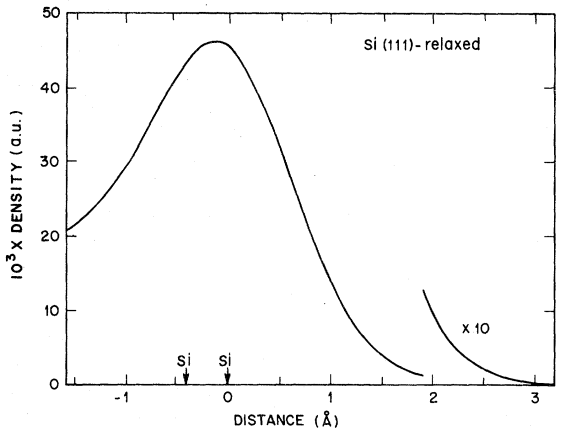

FIG. 4. Planar average electron density for the ideal and relaxed Si(111) surface is plotted versus distance. The origin is chosen at the last Si atom plane. The position of the last two atom planes are indicated by arrows.

for larger z. Comparable information to the above for the hydrogen covered Si(111) surface is plotted in Figs. 5(a), 5(b), and 6. Once again the s band is greatly suppressed outside the surface. Unlike the clean surface, there is no strong structure near the very top of the valence band. The most prominent structure is now near the bottom of the p bands. In fact, there is a significant shift in weight to lower energies in going from the clean to the hydrogenated surface. The shift also manifests itself in the decay rate for the total charge density in the tail region. For H on Si(111), the decay rate $2\kappa = 2\sqrt{2E}$, corresponds to an E of 9.5 eV, placing it near the peak in the spectrum at 4.5 eV in Fig. 5(b) [H-covered Si(111) has an ionization potential ~5.0 eV]. The corresponding energies for clean Si are 7.8 eV, relative to vacuum, and 2.5 eV relative to the valence-band maximum.

We now turn to the task of using the information contained in Figs. 2–5 together with formula (2.11) to calculate the KED spectra shown in Fig. 2.

We begin with clean Si, and the problem of determining the most appropriate values for R and R^*. From work by Hagstrum, the effective ionization energy E_A to be used in (2.12) is ~22.5 eV. This number corresponds to a best estimate of the unbroadened high-energy threshold for the Auger electron distribution corrected by twice the work function of the surface.[15] The difference ΔE between it and the free-atom ionization energy, ~2 eV, represents the relaxation energy associated with the image potential of the free ion near the surface. Using the bulk dielectric constant of Si, $\epsilon \sim 12$ and

$$\Delta E = \frac{\epsilon - 1}{\epsilon + 1}\frac{3.6}{z}\ (\text{eV})\ , \qquad (3.1)$$

(z measured in angstroms) one obtains for $z \sim 1.5$ Å. This distance, however, does not unambiguously fix z relative to the Si lattice, only relative to an effective dielectric surface for which (3.1) is valid. Studies of the effective dielectric surface have only been made for simple model surfaces.[21,22] They imply that for these surfaces a dielectric origin in a region where the density of electrons is reduced to ~$\frac{1}{3}$ its bulk value.[21] For clean Si this would be ~1.2 Å outside the last layer of Si atoms, and place R at 2.7 Å. It must be kept in mind, however, that Si is an open lattice, and that it might be more appropriate to measure z in (3.1) from the last Si layer. R would then be ~1.5 Å. The density of states in these two regions are not very different, as can be seen from Fig. 3(a).

Turning to the problem of locating R^*, there are two limiting assumptions one can make: The first assumes $R^* = R$, i.e., the longitudinal photon is

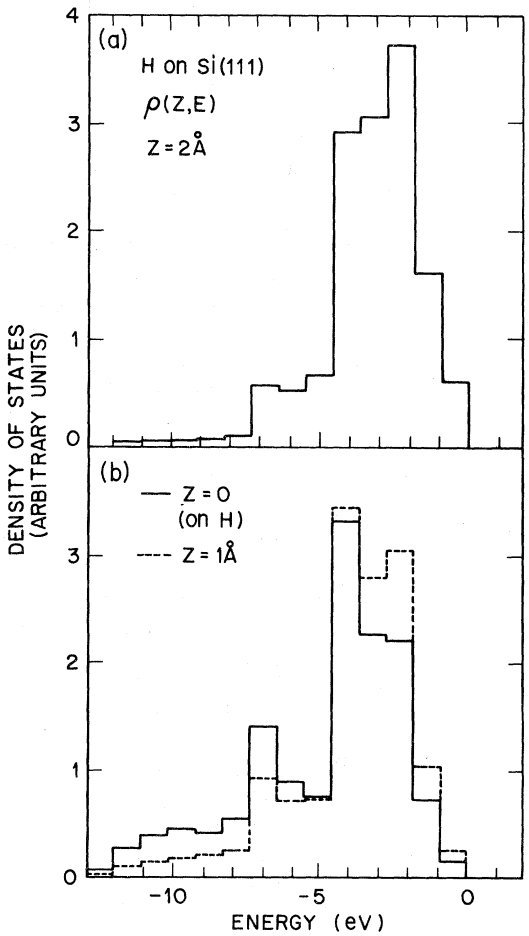

FIG. 5. Planar average density of states for H-covered Si(111) is plotted versus energy (measured from the top of the bulk valence band). (a) For a positon 2 Å above the H layer, (b) for two positions, one on the H layer and the other 1 Å above it.

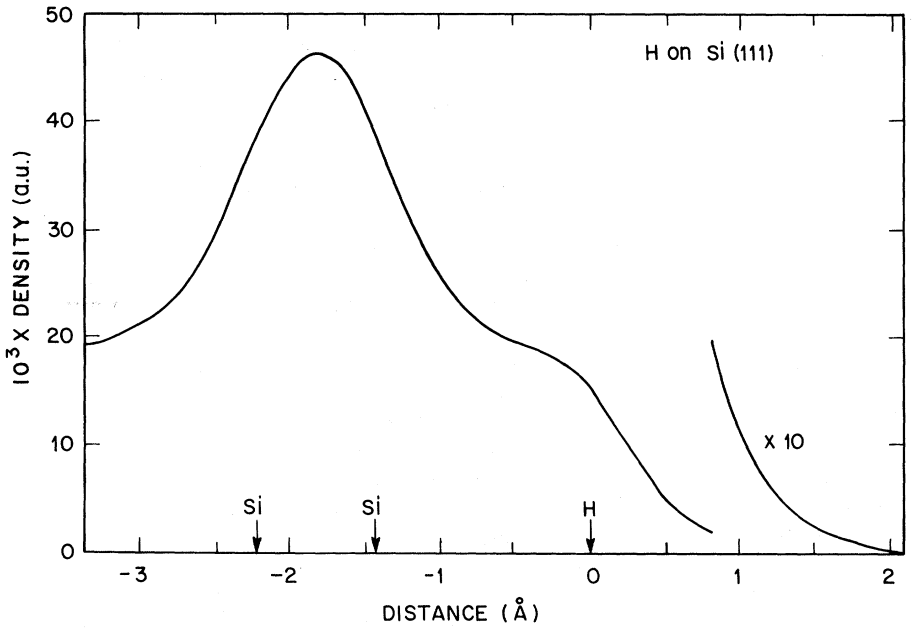

FIG. 6. Planar average total electron density for the H covered Si(111) surface is plotted versus distance. The positions of two Si and the one H layer in the surface region are marked by arrows. Distance is measured relative to the H layer.

absorbed at the same position it is created. The second, that the Auger electron is created in the surface region where the electron density is high and therefore not greatly different from the bulk.

Using (2.11) with $R^* = R$, one sees that $N(E)$ is a self-convolution of the surface density of states modulated by the product of an effective escape probability with a Coulomb matrix element. We focus here on the convolution, plotted in Fig. 7 for $R = 1.7$ and 2.8 Å. The zero of energy is defined as the energy that an Auger electron would have assuming that both holes are at the top of the valence band and that the Auger process is totally adiabatic. The only Auger electrons with kinetic energy greater than zero involve either one or two holes in the dangling bond surface state band. The large peak above zero in Fig. 7 corresponds to creating two holes in the dangling bond band. The second most prominant structure is at -1.5 eV, and involves one hole in the p band and one in the dangling bond band.

Neither curve in Fig. 7 looks like experiment. The most striking difference is the absence, experimentally of the dangling bond peak. A plausible explanation of this is easily arrived at, and illustrates the limitations inherent in (2.12). The dangling bond band is narrow (~ 0.5–1 eV) and only half occupied. Because of electron correlations it is extremely difficult to extract from such a band two electrons from the same spatial region.[23] They must in fact be taken from spatially different regions of the surface—that is, from atomiclike states above the different surface atoms. This is not true of other states for which double occupancy combined with relatively large bandwidth usually insures the availability of two spatially adjacent electrons. This difference strongly suppresses the high-energy peak, in the ratio of the square of the Coulomb field between atoms $(\frac{1}{7})^2$ to that of the Coulomb field at the ion $(1)^2$. This factor of ~ 50 strongly suppresses the dangling bond peak for the self-convolution.

While the above argument removes the high-energy discrepancy between Figs. 7 and 2 the theoretical line shape is still very different from experiment. In particular, the peak at -1.5 eV in Fig. 7 corresponds poorly to the experimental peak which occurs at -4.5 relative to the unbroadened experimental threshold.

For R^* in the bulklike region of the surface, $N(E)$ becomes proportional to a crossfold of a bulklike density of states and a state density a few angstroms outside the surface. Two such crossfolds are plotted in Fig. 8 and correspond to choosing for $\rho(R^*)$ the bulk density of states and for $\rho(R)$ the curves plotted in Fig. 4 for $R = 1.7$ and 2.8Å. The peak previously at -1.5 eV has now shifted lower in energy lying at -3.5 eV. The peak at -6 eV in the theoretical curves we believe is reflected in the experimental curves by the plateau in Fig. 2. The two sets of theoretical curves plotted in Figs. 7 and 8 represent limiting behavior. Of these two extremes we believe the crossfold is to be clearly preferred. Additional support for this conclusion comes from plotting $\rho(R_z^*)\,|\,W(R_z^* - R_z)\,|^2$ vs R_z^* for $R_z = 2.8$ Å. This plot is shown in Fig. 9 and one sees that it certainly favors the region near the surface atoms, not $R_z = R_z^*$. For $|\,W(z - z^*)\,|^2$ we have

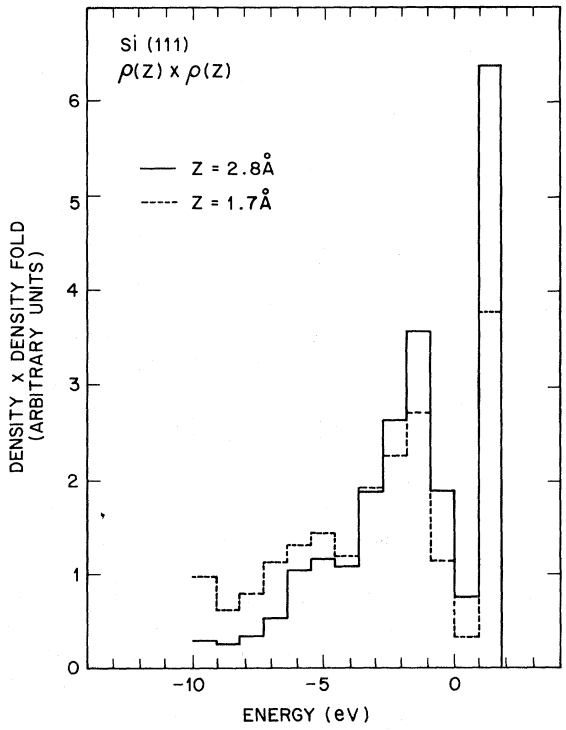

FIG. 7. Density-density self-fold (see text) at two locations (in reference to last Si layer) is plotted versus energy for clean Si(111). The zero of energy is defined at that energy where the top of the valence band folds against itself.

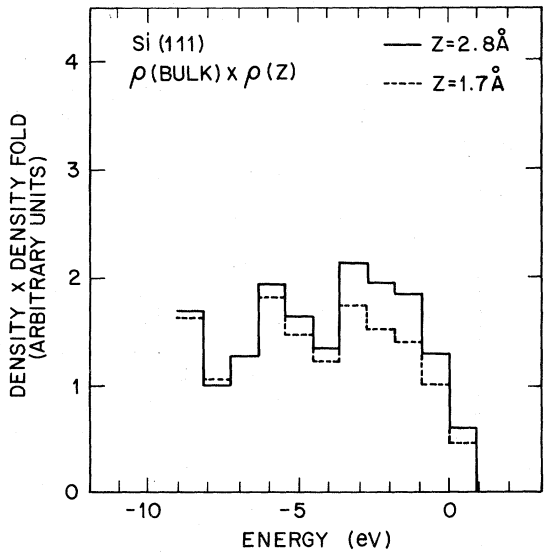

FIG. 8. Crossfold of the bulk Si density of states with two planar averaged denstiies of states is plotted versus energy. The planes are located 1.7 and 2.8 Å from the last Si plane. The zero of energy reference is defined in the Fig. 7 caption.

used $[(z^* - z)^2 + \lambda^2]^{-1}$, where λ is introduced to cut off the Coulomb field near the ion. We choose $\lambda \sim 0.5$, comparable to the spatial extent of the He wave function.

The theoretical analysis for the H-covered Si(111) proceeds in a fashion parallel to that already given for the clean surface. The position-dependent densities of states on various planes at and above the H overlayer have already been discussed and are plotted in Fig. 5. The H overlayer clearly causes significant changes from the clean Si spectra.

The same wide choice presents itself in choosing regions R and R^* to use in (2.12). Rather than attempt to extract the "unbroadened" high-energy threshold from the experimental KED in this case, we shall take as a working hypothesis the assumption that the effective ionization energy $E_A(R)$ is the same as it is for clean Si. This is plausible if the most probable R for neutralization and the location of the effective dielectric surface both depend primarily on electron density. Since the decay rate of the planar average charge is not grossly different for the two surfaces, this would make the image potential or relaxation shift similar. The similarity of E_A for both Ni and Si[1] supports this hypothesis. We shall therefore assume that R is ~ 2 Å outside the last atom layer (in this case the H layer), and, on the basis of our previous comparison, that R^* is within the last layer.

The crossfolds of the state density on the H layer with those 1 and 2 Å outside this layer are shown in Fig. 10. If we ignore the small increase in ionization potential (~ 0.2 eV) found at saturated coverage,[24] this plot and the preferred result for clean Si (the solid curve in Fig. 8) have a common energy scale and can be compared directly. The most sig-

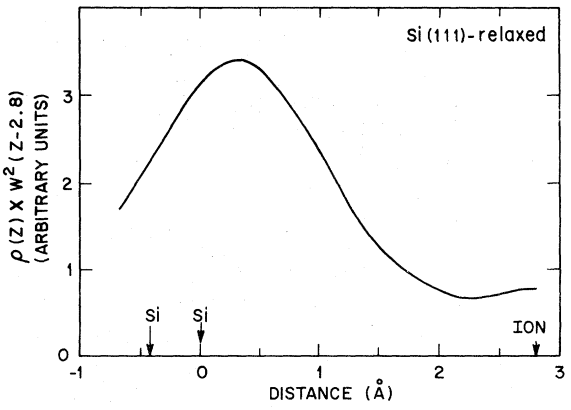

FIG. 9. Product of the electron density with the square of the Coulomb interaction energy $[(z-2.8)^2+0.25]^{-1}$ is plotted versus distance z for relaxed Si(111). The Si atom planes are indicated by arrows as is the ion position at 2.8 Å.

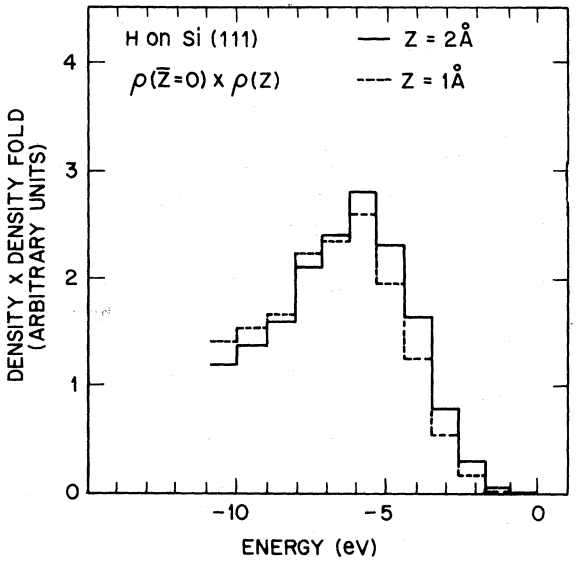

FIG. 10. Crossfold of the planar average density of states at the H with a similar state density located 1 and 2 Å outside the H is plotted versus energy. The surface is H-covered Si(111). The energy reference is defined in the caption of Fig. 7.

nificant differences of the theoretical results for the clean and hydrogenated surfaces are the shift of the peak by ~ 3 eV and the almost total depletion of the top 2–3 eV of the distribution. These are precisely the changes seen in the experimental data in Fig. 2.

The excellent agreement between theory and experiment supports our hypothesis that the effective ionization energy E_A is essentially unchanged. However, note that linearly extrapolating the high-energy side of the theoretical KED in Fig. 10 to zero gives an apparent threshold in error by ~ 2 eV. There is so little weight in the first 2 eV that it could not be experimentally distinguished from a broadened tailing of the lower energy portion of the distribution. This observation explains the unaccountably large apparent shift in E_a which one obtains by applying the extrapolation procedure to the data. Linear extrapolation should give approximately the correct threshold for clean Si, as may be seen from Fig. 8. Therefore this procedure should be applied with caution. As a rule of thumb, we suggest that when the extrapolated threshold gives an image potential shift significantly greater than the usual 2 eV, it is probably wrong.

For comparison, we show in Fig. 11 the self-folds of the state densities at 2 and 1 Å for the hydrogen-covered surface. The differences between these curves and the crossfolds shown in Fig. 10 are much less pronounced than for clean Si. The self-fold at 2 Å, the preferred R, is in somewhat poorer agreement with experiment because the peak shift is too small, but the 1 Å self-fold is essentially indistinguishable from the 2 Å-0 Å crossfold. This suggests that $\rho(1)$ is close to the "convolution mean" of $\rho(0)$ and $\rho(2)$ in this case.[25]

IV. SUMMARY AND CONCLUSIONS

We have in this paper succeeded in calculating theoretically for the first time the kinetic energy distribution of Auger-emitted electrons produced during ion neutralization at a surface.

Two essential ingredients entered this calculation—the first, an expression for the Auger current density $N(E)$, such as (2.12), and second, a knowledge of the position-dependent densities of states for the two surfaces studied. The success of the calculation tends to reinforce our confidence in both. In particular, the independent-particle reasoning that entered the derivation of (2.5) appears justified and the potentially serious effects of hole-hole interactions in the final state of the neutralization event do not seem to play an important role. These hole-hole interactions would presumably manifest themselves by having the experimental peaks in the KED spectra lie considerably lower in energy than would be predicted by Eq. (2.12). We have also presented evidence for the importance of electron correlations in the dangling bond band. Because of its narrow width and partial occupancy, final states in which it contains two holes are much less probable than would be implied by (2.12).

Another question of continuing interest on which

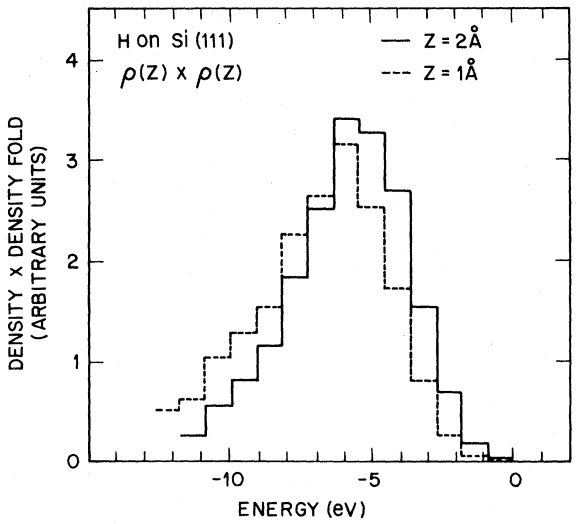

FIG. 11. Self-fold of the planar average density of states at two locations (1 and 2 Å from the H) is plotted versus energy. Energy reference is defined in the caption of Fig. 7.

we have shed some light involves the spatial regions from which the neutralizing and Auger electrons come. The evidence of these calculations supports the position that the Coulomb field acts over a substantial distance, and while the neutralizing electron must tunnel 2 to 3 Å out from the surface layer to neutralize the incoming ion, the Auger electron originates in a region of high density, the last few surface layers.

This suggests a potentially simplifying alternative to the usually deconvolution procedures used in conventional ion-neutralization spectroscopy (INS), at least for clean surfaces. Rather than assuming $R^* = R$ in (2.12) and inverting the nonlinear integral equation for $\rho(R, E)$ that (2.12) becomes, one would use for $\rho(R^*, E)$ the bulk density of states. Equation (2.12) then becomes a linear integral equation for $\rho(R, E)$ that is relatively easy to solve, and not as subject to numerical instabilities as the nonlinear equation. It should be interesting to compare the two approaches. In situations where $\rho(z, E)$ as a function of z maintains its shape (as a function of energy) from the surface atom layer into the vacuum region [as was the case for H chemisorbed on Si(111)] the two methods should yield similar results. $\rho(R, E)$ extracted from the linear equations would represent the density of states near the ion, while that extracted from the nonlinear equations would be representative of an intermediate region between the ion and the surface layer. For cases where the density of states function does not maintain its shape through the surface region, there may be interesting differences between the two approaches.

ACKNOWLEDGMENTS

We should like to thank Dr. H. D. Hagstrum and Dr. T. Sakurai for numerous useful discussions and for making available to us (before publication) the experimental data contained in Fig. 2.

[1]H. D. Hagstrum, Phys. Rev. 96, 336 (1954).
[2]H. D. Hagstrum, Phys. Rev. 122, 83 (1961).
[3]H. D. Hagstrum and G. E. Becker, Phys. Rev. 159, 572 (1967).
[4]H. D. Hagstrum, Journal Res. Natl. Bur. Stand. A 74, 433 (1970); *Metals*, edited by R. F. Bunshah (Wiley, New York, 1972), Vol. 6, p. 309.
[5]H. D. Hagstrum and G. E. Becker, Phys. Rev. 8, 1580 (1973).
[6]H. D. Hagstrum and G. E. Becker, J. Chem. Phys. 54, 1015 (1971).
[7]H. D. Hagstrum and G. E. Becker, in Proceedings of the Battelle Colloquium on the Physical Basis for Heterogeneous Catalysis, Gstaad, Switzerland, 1974 (Plenum, New York, to be published).
[8]J. A. Appelbaum and D. R. Hamann, Phys. Rev. Lett. 32, 225 (1974).
[9]J. A. Appelbaum and D. R. Hamann, Phys. Rev. Lett. 34, 806 (1975).
[10]H. D. Hagstrum, Phys. Rev. 122, 83 (1961).
[11]W. E. Spicer, Phys. Rev. 112, 114 (1958).
[12]W. L. Schaich and N. W. Ashcroft, Phys. Rev. B 3, 2452 (1971); G. D. Mahan, *ibid.* 2, 4334 (1970); I. Adawi, Phys. Rev. 134, A788 (1964).
[13]E. H. S. Burhop, *The Auger Effect and Other Radiationless Transitions* (Cambridge U. P., London, 1972).
[14]V. Heine, Phys. Rev. 151, 561 (1966).
[15]This effect, currently referred to as relaxation (Ref. 16), was first discussed by H. D. Hagstrum (Ref. 1).
[16]J. E. Demuth and D. E. Eastman, Phys. Rev. Lett. 32, 1123 (1974); D. A. Shirley, Chem. Phys. Lett. 22, 301 (1973); P. H. Citrin and D. R. Hamann, *ibid.* 22, 301 (1973).
[17]H. D. Hagstrum, Y. Takeishi, and D. D. Pretzer, Phys. Rev. 139, 526 (1965); H. D. Hagstrum and Y. Takeishi, *ibid.* 137, 304 (1965).
[18]T. Sakurai and H. D. Hagstrum, Phys. Rev. B (to be published).
[19]J. E. Florio and W. D. Robertson, Surf. Sci. 24, 17 (1971).
[20]J. E. Rowe and H. Ibach, Phys. Rev. Lett. 31, 102 (1973).
[21]J. A. Appelbaum and D. R. Hamann, Phys. Rev. B 6, 1122 (1972).
[22]N. D. Lang and W. Kohn, Phys. Rev. B 7, 3541 (1973).
[23]This effect was independently suggested by V. Heine (private communication).
[24]T. Sakurai and H. D. Hagstrum (unpublished).
[25]H. D. Hagstrum and G. E. Becker, Phys. Rev. B 4, 4187 (1971).